



Original Article

Superior stemness of a rapidly growing subgroup of isolated human auricular chondrocytes and the potential for use in cartilage regenerative therapy



Reina Shimizu ^a, Yukiyo Asawa ^b, Makoto Komura ^b, Kazuto Hoshi ^{a, b, c}, Atsuhiko Hikita ^{b, *}

^a Department of Sensory and Motor System Medicine, Graduate School of Medicine, The University of Tokyo, 7-3-1 Hongo, Bunkyo-ku, Tokyo 113-8655, Japan

^b Division of Tissue Engineering, The University of Tokyo Hospital, 7-3-1 Hongo, Bunkyo-ku, Tokyo 113-8655, Japan

^c Department of Oral-maxillofacial Surgery, Dentistry and Orthodontics, The University of Tokyo Hospital, 7-3-1 Hongo, Bunkyo-ku, Tokyo 113-8655, Japan

ARTICLE INFO

Article history:

Received 11 October 2021

Received in revised form

15 December 2021

Accepted 20 December 2021

Keywords:

Cartilage regenerative medicine

Chondrocytes

Cell division rate

Flow cytometry

Cell preparation

Microarray analysis

ABSTRACT

Introduction: In cartilage regenerative medicine, transplanted chondrocytes contain a mixture of populations, that complicates the regeneration of uniform cartilage tissue. Our group previously reported that chondrocytes with higher chondrogenic ability could be enriched by selection of rapidly growing cells. In this study, the detailed properties of rapidly growing chondrocytes were examined and compared to slowly growing cells.

Methods: Human auricular chondrocytes were fluorescently labeled with carboxyfluorescein succinimidyl ester (CFSE) and analyzed using flow cytometry, focusing on division rates as indicated by fluorescence intensity and cell morphology according to the forward scatter and side scatter. Rapid and slow growing cell groups were harvested on days 2 and 4 after CFSE labeling, and their ability to produce cartilage matrix *in vitro* was examined. To compare the chondrogenic ability *in vivo*, the cells were seeded on poly-L-lactic acid scaffolds and transplanted into nude mice. Gene expression differences between the rapid and slow cell groups were investigated by microarray analysis.

Results: On day 2 after CFSE labeling, the rapidly growing cell group showed the highest proliferation rate. The results of pellet culture showed that the rapid cell group produced more glycosaminoglycans per cell than the slow cell group. The amount of glycosaminoglycan production was highest in the rapid cell group on day 2 after CFSE labeling, indicating high chondrogenic ability. Furthermore, microarray, gene ontology, and Kyoto Encyclopedia of Genes and Genomes pathway analyses showed upregulation of genes that promote cell division such as origin recognition complex subunit 1 and downregulation of genes that inhibit cell division such as cyclin dependent kinase inhibitor 1A. Besides cell cycle-related genes, chondrocyte-related genes such as serpin family B member 2, clusterin, bone morphogenetic protein 2, and matrix metalloproteinase 3 were downregulated, while fibroblast growth factor 5 which is involved in stem cell maintenance, and coiled-coil and C2 domain containing 2A, which is required for cilia formation, were upregulated.

Conclusion: The results showed that the rapid cell group proliferated well and had more undifferentiated properties, suggesting a higher stemness. The present findings provide a basis for the use of the rapid cell group in cartilage regeneration.

© 2022, The Japanese Society for Regenerative Medicine. Production and hosting by Elsevier B.V. This is an open access article under the CC BY-NC-ND license (<http://creativecommons.org/licenses/by-nc-nd/4.0/>).

Abbreviations: CFSE, carboxyfluorescein succinimidyl ester; FC, fold change; GAG, glycosaminoglycan; PLLA, poly-L-lactic acid.

* Corresponding author. Fax: +81-3-5800-9891.

E-mail address: ahikita-ky@g.ecc.u-tokyo.ac.jp (A. Hikita).

Peer review under responsibility of the Japanese Society for Regenerative Medicine.

<https://doi.org/10.1016/j.reth.2021.12.005>

2352-3204/© 2022, The Japanese Society for Regenerative Medicine. Production and hosting by Elsevier B.V. This is an open access article under the CC BY-NC-ND license (<http://creativecommons.org/licenses/by-nc-nd/4.0/>).

1. Introduction

Cartilage is a non-vascular tissue with limited ability for self-repair. The clinical application of cartilage regeneration medicine has been progressing over the past decades. In 1994, Brittberg et al. reported a method of autologous chondrocyte implantation for the treatment of localized defects of articular cartilage [1,2]. In 2006, a

transplantation technique in which a suspension containing autologous cultured chondrocytes was injected subcutaneously above the nasal septum was reported. This method is applicable in the field of plastic and cosmetic surgery [3]. In other work, our research group have previously developed an implantable tissue-engineered cartilage using poly-L-lactic acid (PLLA) scaffolds. In a clinical study, this cartilage was subcutaneously inserted into the dorsal nasal surface of three patients to correct cleft lip and nose deformities [4]. Three-dimensional data from computed tomography images showed effective augmentation over almost the entire length of the dorsal nasal surface, as observed in the medial line of the face. The effect was maintained for 1 year postoperatively, and the curve of the nasal dorsum was unaffected during the observation period.

Cell expansion culture is a necessary step in order to obtain a sufficient number of cells for such work as described above. In our clinical study, the number of chondrocytes was eventually increased to 240 million cells after 4 weeks of culture [4]. However, during long-term monolayer culture and repeated passaging, chondrocytes lose their ability to produce cartilaginous matrices, such as glycosaminoglycans (GAG) and type II collagen (COL2); instead, they begin to produce type I collagen (COL1). This process is termed dedifferentiation [5,6]. In turn, dedifferentiated chondrocytes regain their ability to produce matrix proteins after transplantation and regenerate cartilage.

It is also noteworthy that transplanted chondrocytes contain a mixture of populations, possibly due to the heterogeneity of cells in cartilage tissues or because of differences in the extent of dedifferentiation during culture [7–10]. This heterogeneity in chondrocytes complicates the regeneration of uniform cartilage tissue. In our previous report, the regenerated cartilage tissue produced from human auricular chondrocytes showed an islet-like appearance [11,12]. To address these issues, some research groups have selected highly chondrogenic cells using cell surface markers [13–15]. However, this method is unreliable because cell surface markers may change depending on culture conditions and the number of passages [16,17].

We previously reported that chondrocytes that showed a rapid decrease in cell labeling with carboxyfluorescein succinimidyl ester (CFSE) – indicating a higher division rate – were more likely to produce substrates than those with a slow decrease [18]. Furthermore, cells with a higher rate of division tended to have uniform side scatter (SSC) which is a measure of internal structure and smaller forward scatter (FSC) which is a measure of cell size relative to cells with a slow division rate on day 4 of proliferation. This suggests that different populations of cells are present in the rapidly/slowly dividing groups. These results indicate that selection of chondrocytes according to their division rate could be a promising approach for improving the reliability and quality of regenerated cartilage. However, the reasons responsible for the high chondrogenic capacity of rapidly dividing cells has not been determined and improved cartilage regeneration may depend on the high proliferation rate or other unique characteristics of the rapidly dividing cells. It is therefore important to characterize in detail the properties of the rapidly growing cells.

The purpose of this study was to define the characteristics of rapidly and slowly dividing cells in terms of their morphology, numbers of divisions, and gene expression patterns.

2. Materials and methods

2.1. Isolation of human auricular chondrocytes

The use of human auricular chondrocytes for research was approved by the Research Ethics Committee of The University of

Tokyo Hospital (ethical approval numbers: 622, 2573, and 2019094NI). Patients with microtia provided informed consent for the harvest of human auricular cartilages during surgery at Nagata Microtia and Reconstructive Plastic Surgery Clinic. Soft tissues and perichondria were removed from auricular cartilage, and minced auricular cartilage was incubated with 0.3% collagenase solution in a shaker bath at 37 °C for 18 h. After filtration with a cell strainer (pore size: 100 µm; BD Falcon, Tokyo, Japan), human auricular chondrocytes were collected by centrifugation at 440g for 5 min. Subsequently, 2×10^5 chondrocytes were cultured in Dulbecco's modified Eagle's medium/nutrient mixture F-12 (DMEM/F12; Sigma–Aldrich Co.) supplemented with 5% human serum (Sigma–Aldrich Co.), 100 ng/mL FGF-2 (Kaken Pharmaceutical Co, Ltd.), 5 µg/mL insulin (Novo Nordisk Pharma Ltd.), and 1% penicillin/streptomycin (Sigma–Aldrich Co.) (cartilage growth medium) in ϕ 100 mm COL1-coated dish (AGC Techno Glass Co., Ltd.) at 37 °C in a humidified atmosphere containing 5% CO₂. When cells reached confluence (i.e., after 7 days), they were harvested using trypsin-EDTA (Sigma–Aldrich Co.), centrifuged, resuspended in CELL-BANKER (Nippon Zenyaku Kogyo Co., Ltd.), and stored at –80 °C.

2.2. Cell labeling with CFSE

The frozen cell stocks were thawed and cultured (passage 1 [P1]) in chondrocyte growth medium for 7 days in an incubator at 37 °C and 5% CO₂. Cells were then harvested and labeled with the Cell-Trace™ CFSE Cell Proliferation Kit (Thermo Fisher Scientific Inc.) according to the instructions provided by the manufacturer. After confirming that the cells were fluorescently labeled using a BD LSRFortessa™ instrument (Becton, Dickinson and Co.), the labeled chondrocytes were seeded onto culture dishes (P2). Cell numbers and viability were checked using CellDrop™ Automated Cell Counters (DeNovix, USA) or a Bürker-Türk counting chamber (ERMA Inc., Tokyo, Japan). Microscopic observation of the cells was performed using a Leica DM IL (Leica Microsystems K.K.).

2.3. Selective isolation of target cells

CFSE-labeled chondrocytes were sorted on day 2 or 4 of P2 culture using a BD FACSAria™ Fusion instrument (Becton, Dickinson and Co.) The top 30% fluorescently labeled cells were collected and assigned as the slow cell group. The bottom 30% of fluorescently labeled cells were assigned as the rapid cell group.

2.4. Cell Counting Kit-8 (CCK-8) assay

To examine the cell proliferation, fluorescence-activated cell sorting-sorted (FACS-sorted) chondrocytes were seeded at a density of 2×10^3 cells/well into a type 1 collagen (COL1)-coated 96-well microplate (AGC Techno Glass Co., Ltd.) and cultured in cartilage growth medium for 1, 3, 5, and 7 days, respectively. After replacing the medium with DMEM/F12 (100 µL) (Sigma–Aldrich Co.) supplemented with 1% penicillin/streptomycin (Sigma–Aldrich Co.) (i.e., basic medium), CCK-8 solution (10 µL) was added to each well, and the cells were cultured for 1.5 h in an incubator at 37 °C and 5% CO₂. Cell activity was evaluated using a CCK-8 kit (Dojindo, Kumamoto, Japan) according to the instructions provided by the manufacturer. The absorbance of the sample solution at 450 nm was measured using a microplate reader (ARVO X3; PerkinElmer Co., Ltd., USA).

2.5. Evaluation of cartilage regeneration in vitro

Human auricular chondrocytes from the rapid or slow cell groups were suspended in 1% atelocollagen at a concentration of

1×10^7 cells/mL. The cell-collagen mixture (20 μ L) was placed at the bottom of a 15 mL conical tube (BD Falcon, USA) and incubated for 2 h at 37 °C and 5% CO₂. Differentiation medium (2 mL) (DMEM/F12 supplemented with insulin-like growth factor-1 [IGF-1]; 1 μ g/mL; Astellas Pharma Inc. Tokyo, Japan) was added after gelation, and the cells were cultured for 3 weeks in an incubator at 37 °C and 5% CO₂.

2.6. Evaluation of cartilage regeneration in vivo

All animal experiments were performed under the ethical guidance of the University of Tokyo (ethics approval numbers: P14-104, P15-019, and P19-114). Chondrocyte suspension in 1% atelocollagen solution (1×10^7 cells/mL) was loaded onto PLLA scaffolds (5 × 5 × 3 mm) (GC R&D Dept, Tokyo, Japan), and cultured for 2 h at 37 °C and 5% CO₂ to prepare cartilage regeneration constructs. Six-week-old male BALB/cAJcl-nu/nu mice (Nippon Bio-Supp. Center) were used for transplantation. Mice were anesthetized by inhalation of 2% isoflurane (AbbVie). The skin of the mice was sterilized with 70% ethanol, and an incision was performed slightly below the midline of the back using scissors. The subcutaneous tissue was detached with abrasive scissors, and cartilage constructs were implanted under the back skin. The incision was sutured with two stitches using 5-0 nylon. Grafts were collected and halved at 2, 4, and 8 weeks after implantation and used for GAG measurements and histological analyses.

2.7. Biochemical analyses

The minced samples were digested by incubation in 10 mg/mL pepsin and 0.05 M acetic acid at 4 °C. After 48 h, 1 mg/mL pancreatic elastase and 10 × tris-buffered saline (TBS) were added to the solution, and the samples were incubated at 4 °C overnight. Subsequently, the samples were centrifuged at 12,000 g for 5 min to remove the debris. GAGs in the supernatants were quantified using a Blyscan Glycosaminoglycan Assay Kit (Biocolor Ltd., United Kingdom) according to the instructions provided by the manufacturer.

2.8. Cell proliferation assay

At P2, human auricular chondrocytes were labeled using CFSE. After labeling, the cells were cultured and harvested on days 2 and 4, and the CFSE fluorescence intensity was measured using flow cytometry to determine the proliferative potential of the chondrocytes. Data were analyzed with FlowJo™ software (Becton, Dickinson and Co.).

2.9. Microarray gene expression profiling

Total RNA was extracted from the rapid and slow cell groups isolated under the aforementioned conditions on day 2 after CFSE labeling. The cDNA was synthesized using the GeneChip WT (Whole Transcript) Amplification kit according to the instructions provided by the manufacturer. The sense cDNA was subsequently fragmented and biotin-labeled with terminal deoxynucleotidyl transferase using the GeneChip WT Terminal labeling kit. Labeled DNA targets were hybridized overnight to the Affymetrix GeneChip Array. The arrays were washed, stained on a GeneChip Fluidics Station 450, and scanned using a GCS3000 Scanner (Affymetrix). Computation of the probe cell intensity data and generation of a CEL file were performed using the Affymetrix® GeneChip Command Console® software (AGCC).

2.10. Gene ontology (GO) and pathway analysis

The data were summarized and normalized with Signal Space Transformation-Robust Multichip Analysis (SST-RMA) method implemented in Affymetrix® Power Tools (APT). We exported the result with gene level SST-RMA analysis and performed the differentially expressed gene (DEG) analysis. For a DEG set, hierarchical cluster analysis was performed using complete linkage and Euclidean distance as a measure of similarity. Gene Ontology (GO) (<http://geneontology.org>) and Kyoto Encyclopedia of Genes and Genomes (KEGG) (<http://kegg.jp>) were used to analyze the significant probe list for gene enrichment and functional annotation. For GO analysis, we used gProfiler to calculate the GO term corresponding to a false discovery rate (FDR) < 5% that was controlled by adjusting p-values using the Benjamini-Hochberg algorithm. For KEGG analysis, p-values were calculated using a modified fisher's exact test and all FDR and Bonferroni values were calculated. All data analysis and visualization of differentially expressed genes were conducted using the software R 3.3.2.

2.11. Isolation of RNA and real-time quantitative polymerase chain reaction (qPCR)

Total RNA was isolated from the collected samples using ISOGEN (Nippon Gene Co., Ltd, Tokyo, Japan) according to the instructions provided by the manufacturer. RNA was reverse transcribed using the PrimeScript™ reagent Kit (TAKARA Bio Inc., Tokyo, Japan). Gene expression was detected using the THUNDERBIRD® Next SYBR® qPCR Mix (TOYOBO CO., LTD, Tokyo, Japan). Real-time qPCR was performed on a 7500 Fast Real-Time PCR System (Applied Biosystems, CA, USA). All primers were specific for human genes, and the transcript levels were normalized to those of GAPDH (Supplemental Table 1).

2.12. Histology

The collected samples were fixed with 4% paraformaldehyde and embedded in paraffin. The fixed samples were cut into longitudinal sections (thickness: 4.5 μ m) using a microtome (RM2265; Leica) and stained with toluidine blue.

2.13. Statistical analysis

All experiments were conducted using three different lots of cells (n = 3). Comparisons between the four groups at the same time point were performed by Tukey's test from one-way analysis of variance (ANOVA) using the EZR software, version 1.54 [19]. Data are expressed as the mean \pm standard deviation. The multiplicity of tests for the number of time points was corrected by the Bonferroni's test; data obtained at one time point, three time points, and four time points were considered significantly different at P < 0.05, P < 0.0167, and P < 0.0125, respectively. Statistical significance of the gene expression data was determined using a Student's t-test and fold change (FC). Statistically significant differences were defined as |FC| \geq 2 and raw. P < 0.05.

3. Results

3.1. The difference in fluorescence intensity and morphology between the rapid and slow cell groups peaked at different days

In our previous report, morphological differences between rapidly and slowly dividing cells were suggested by the FSC/SSC plot of flow cytometry on day 4 [18]. In the current study, the morphological differences between these two groups were

analyzed over time from day 0 to day 6 in addition to the measurement of CFSE fluorescence intensity. Initially, after CFSE labeling, the 30% most strongly stained and 30% most weakly stained

were assigned to the slow and rapid cell groups, respectively. The top two images included in Fig. 1 show histograms of CFSE staining for all cells and the rapid/slow cell groups. The day of CFSE labeling

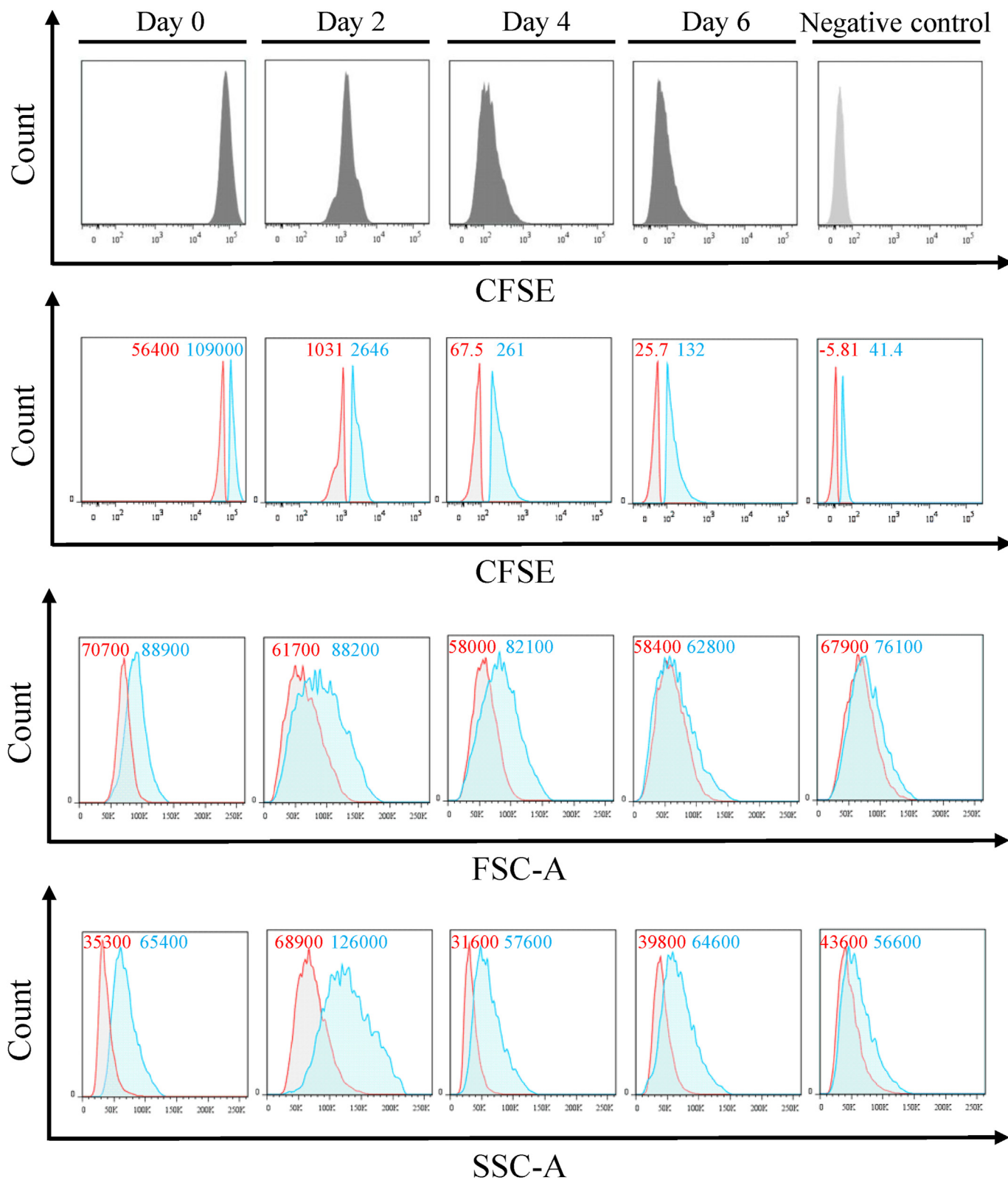


Fig. 1. FACS analysis of fluorescence intensity of CFSE, FSC-A, and SSC-A of human auricular chondrocytes. The day of CFSE staining was set as day 0, and the fluorescence intensity was monitored over time. Upper columns show the CFSE intensity of whole cells, and others indicate CFSE intensity, FSC-A, and SSC-A of rapid (red line) and slow (blue line) cell groups. The median value for each histogram is indicated (red: rapid, blue: slow).

of human auricular chondrocytes was set as day 0, and the decay of fluorescence intensity was monitored over time. The base of the histogram widened the most on day 4 after CFSE labeling, suggesting that the difference in cell division rate increased, thereby facilitating the selection of the rapid and slow cell groups. In contrast, the distance between the peaks in side scatter-area (SSC-A) histograms of the groups was greatest on day 2, whereas those of forward scatter-area (FSC-A) were not separated throughout the analysis period. Based on these results, cells diverged on days 2 and 4 were analyzed hereafter.

3.2. A higher proliferation rate was confirmed for chondrocytes in the rapid cell group

On days 1, 3, 5, and 7 after sorting, the proliferation rate of each group was quantified using the CCK-8 assay. The rapid cell groups sorted on day 2 (day-2 rapid) and day 4 (day-4 rapid) after CFSE labeling had a higher proliferative capacity than the corresponding slow cell groups collected on day 2 (day-2 slow) and day 4 (day-4 slow), respectively. Notably, the day-2 rapid group exhibited the highest capacity for cell proliferation (Fig. 2). Further investigation revealed significant differences between the day-2 rapid and day-2 or day-4 slow groups and day-4 rapid ones and day-2 slow ones on day 5 after sorting. On day 7 after sorting, there were significant differences between day-2 rapid or day-4 slow groups and day-2 or day-4 slow groups, respectively.

3.3. Higher chondrogenic ability was confirmed for the rapid cell groups by *in vitro* pellet culture

Cell pellets of the rapid/slow cell groups were cultured and analyzed to compare their chondrogenic potential. The histological sections stained with toluidine blue after 3 weeks of culture indicated that the cell pellets of the day-2 rapid and day-4 rapid groups were larger and showed more metachromasia than those of the day-2 slow and day-4 slow groups (Fig. 3a). The quantification of GAG revealed that the cell pellets of the day-2 rapid and day-4 rapid groups tended to be higher in GAG content per mg of protein than those of the day-2 slow and day-4 slow groups, respectively, even though there is no significant difference (Fig. 3b). The higher GAG content may be the consequence of the higher cell number in the

rapid cell groups because of the higher division rate. To confirm this hypothesis, the GAG contents were adjusted according to the cell numbers. The results showed that the GAG content per cell also tended to be higher in the rapid cell groups relative to the slow cell groups. GAG accumulation per cell content was significantly higher in the day-2 rapid groups than in the day-4 slow groups. These findings indicate that the chondrogenic ability of each cell in the rapid group was higher than that of cells in the slow cell group (Fig. 3c).

3.4. Highest chondrogenic ability was confirmed for the day-2 rapid group *in vivo*

To evaluate the chondrogenic ability of each group *in vivo*, cells of each group were resuspended in atelocollagen, loaded onto PLLA scaffolds, and transplanted into the back of nude mice. Histological analyses indicated that both the rapid and slow cell groups showed an increase in the metachromasia-positive area over time. Of note, the rapid cell groups tended to show wider metachromasia-positive areas than the slow cell groups at the same time points (Figs. 4a and b).

GAG accumulation per mg of total protein at 2, 4, and 8 weeks after transplantation indicated that all groups showed an increase in GAG over time. The rapid cell group tended to accumulate more GAG than the slow cell group at each stage. At 8 weeks post transplantation, the day-2 rapid group had significantly higher GAG production than the day-2 and 4 slow groups. Furthermore, the day-2 rapid group tended to produce the highest amount of GAG at each stage (Fig. 4c).

3.5. Different generations of cells were included in the rapid/slow cell groups collected on days 2 and 4 after CFSE labeling

Proliferation analyses were performed to compare the numbers of divisions of cells composing the rapid/slow cell groups on days 2 and 4. The group of cells at 4 days after CFSE labeling contained more cells with different division rates than the group of cells at 2 days (Fig. 5a). The day-2 slow group was mainly composed of undivided cells, which remained on day 4 (Fig. 5b). The day-4 slow group was mainly composed of cells that had divided once. This was also true for a substantial part of the day-2 slow group. These

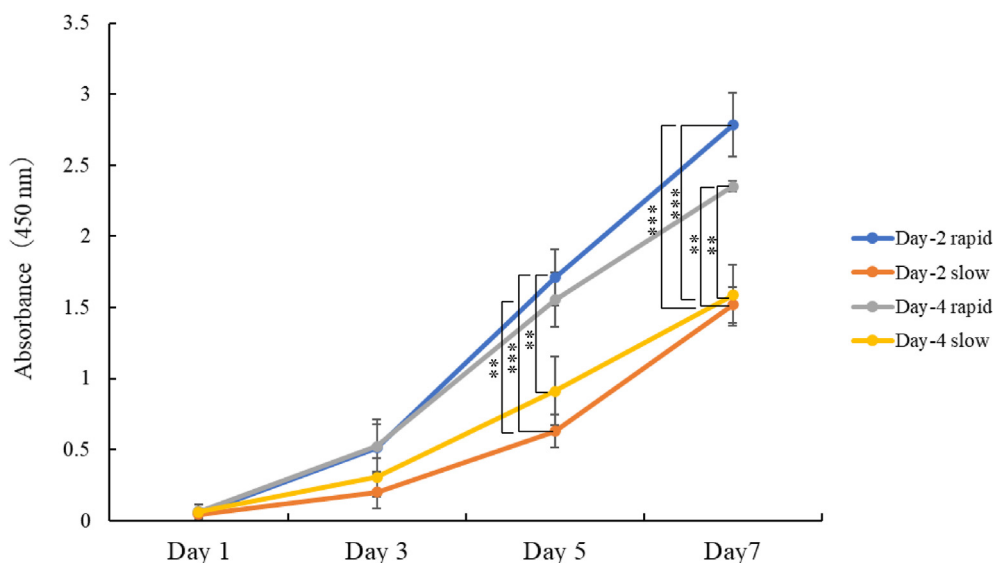


Fig. 2. CCK-8 assay of the rapid/slow cell groups. Cell proliferation of the rapid and slow cell groups sorted on day 2 or 4 was examined by CCK-8 assay on days 1, 3, 5, and 7 ($n = 3$, ** $P < 0.01$, *** $P < 0.001$).

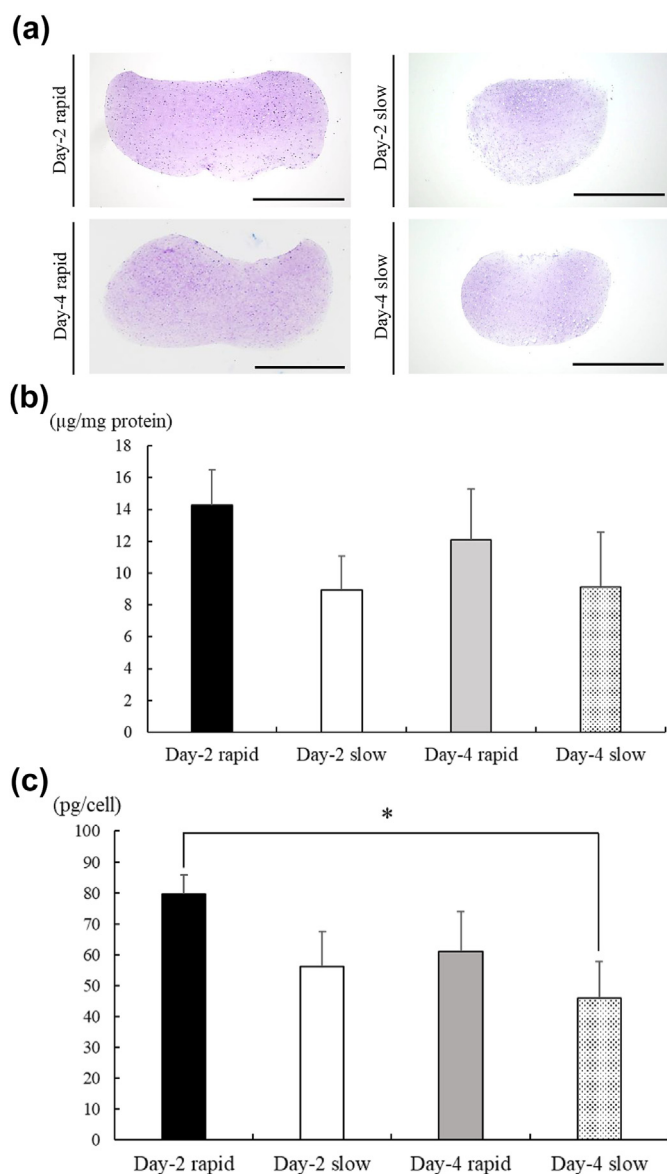


Fig. 3. Evaluation of cartilage regeneration *in vitro* by the rapid and slow cell groups sorted on day 2 or 4. a. Histological analysis of cell pellets after 3 weeks of culture. Samples were stained with toluidine blue. Magnification: $\times 4$; Scale bar: 1,000 μm . b and c. Biochemical analysis. Accumulation of GAG after 3 weeks of culture was examined both per mg total protein (b) and per cell (c) ($n = 3$, $*P < 0.05$).

data indicate that the day-2 slow and day-4 slow groups were similar in terms of generation of cells. In contrast, the day-2 rapid and day-4 rapid groups only shared the cells with three divisions, indicating that the generation of the cell population in both of the rapid cell groups was markedly different (Fig. 5b).

3.6. Rapid and slow cell groups exhibited distinct gene expression

Microarray analyses were performed on cells isolated on day 2 after CFSE labeling to analyze gene expression in the rapid and slow cell groups. A total of 109 genes were differentially expressed in the rapid and slow cell groups with a fold change (FC) value of ≥ 2.0 and a P-value < 0.05 (Fig. 6a). There were 41 upregulated genes and 68 downregulated genes identified. Clustering analyses indicate that the rapid or slow cell groups of three lots had similar gene expression patterns (Fig. 6b).

We performed functional classification by GO and KEGG pathway analyses to further understand the overall function of significant genes. Differentially expressed genes were classified by three major functional types: biological process, cellular component, and molecular function (Fig. 6c). Many of the top 10 terms in the biological process GO functional analysis (Fig. 6c-i) were related to gene expression, chromatin organization, and DNA replication, reflecting the selection of cells according to their division rates. Terms in cellular component (Fig. 6c-ii) and molecular function analyses (Fig. 6c-iii) also included those related to cell division. Terms in the KEGG pathway functional analysis included alcoholism, systemic lupus erythematosus, and viral carcinogenesis, which were consequences of differences in the expression levels of histone genes (e.g., HIST2H2BF, HIST1H2BF). These data reflect the difference in the division rates between groups (Fig. 6d and Supplemental Table 2). The KEGG pathway analysis also revealed that genes related to the p53 signaling pathway and cellular senescence were enriched, suggesting that the state of cellular senescence differs between rapidly and slowly dividing cells.

Finally, to confirm the reliability of the RNA microarray data, real-time qPCR analysis was performed for selected genes from the candidates with $|\text{FC}| \geq 2.0$ and P-value < 0.05 . RNA microarray data showed that the expression levels of origin recognition complex subunit 1 (ORC1), fibroblast growth factor 5 (FGF5), and coiled-coil and C2 domain containing 2A (CC2D2A) were upregulated in day-2 rapid cell groups, while the expression levels of cyclin dependent kinase inhibitor 1A (CDKN1A), serpin family B member 2 (SERPINB2), clusterin (CLU), bone morphogenetic protein 2 (BMP-2), and matrix metalloproteinase 3 (MMP-3) were downregulated. Q-PCR experiments yielded comparable findings to those obtained from the RNA microarray, suggesting that the RNA microarray analysis was highly reliable (Fig. 6e).

4. Discussion

In general, tissue stem cells have a high proliferative potential *in vitro*. It has been reported that cells with strong stem cell characteristics, such as regenerative progenitor cells, divide quickly in low-density cell cultures [13]. It has also been reported that vascular cell adhesion molecule 1 (VCAM-1)-positive human mesenchymal stem cells (MSCs) which have a high rate of mitosis and high cell motility (termed rapidly expanding clones) have strong pluripotency and self-renewal ability [20]. A different research group reported that chondrocyte progenitor cells can be obtained by low-glucose and low-density culture, and that cartilage regeneration was improved in transplantation experiments with these cells [21]. We hypothesized that rapidly dividing chondrocytes also possess stem-like features that enable better chondrogenesis relative to slowly dividing cells.

Because stem cells tend to be smaller with a round shape [22], in this study, as well as CFSE fluorescence intensity decay we examined FSC and SSC, which are FACS indicators of cell morphology. We found that both FSC-A and SSC-A tended to be lower in the rapid cell group, indicating a smaller size and less granularity of this group of cells (Fig. 1). This difference in SSC-A between the groups appeared to be greatest at day 2. In contrast, the width of the histogram was greatest at day 4, suggesting the greatest difference in the cell division number of cells at both ends of the histogram. In fact, the numbers of divisions of the rapid and slow groups did not overlap for day 4 cells, while partial overlap was observed between both groups of day 2 cells (Fig. 5).

The proliferation rate and chondrogenic ability of cells were compared 2 and 4 days after CFSE labeling. The comparison demonstrated that the rapid group harvested at both 2 days and 4 days tended to be more proliferative and chondrogenic than the

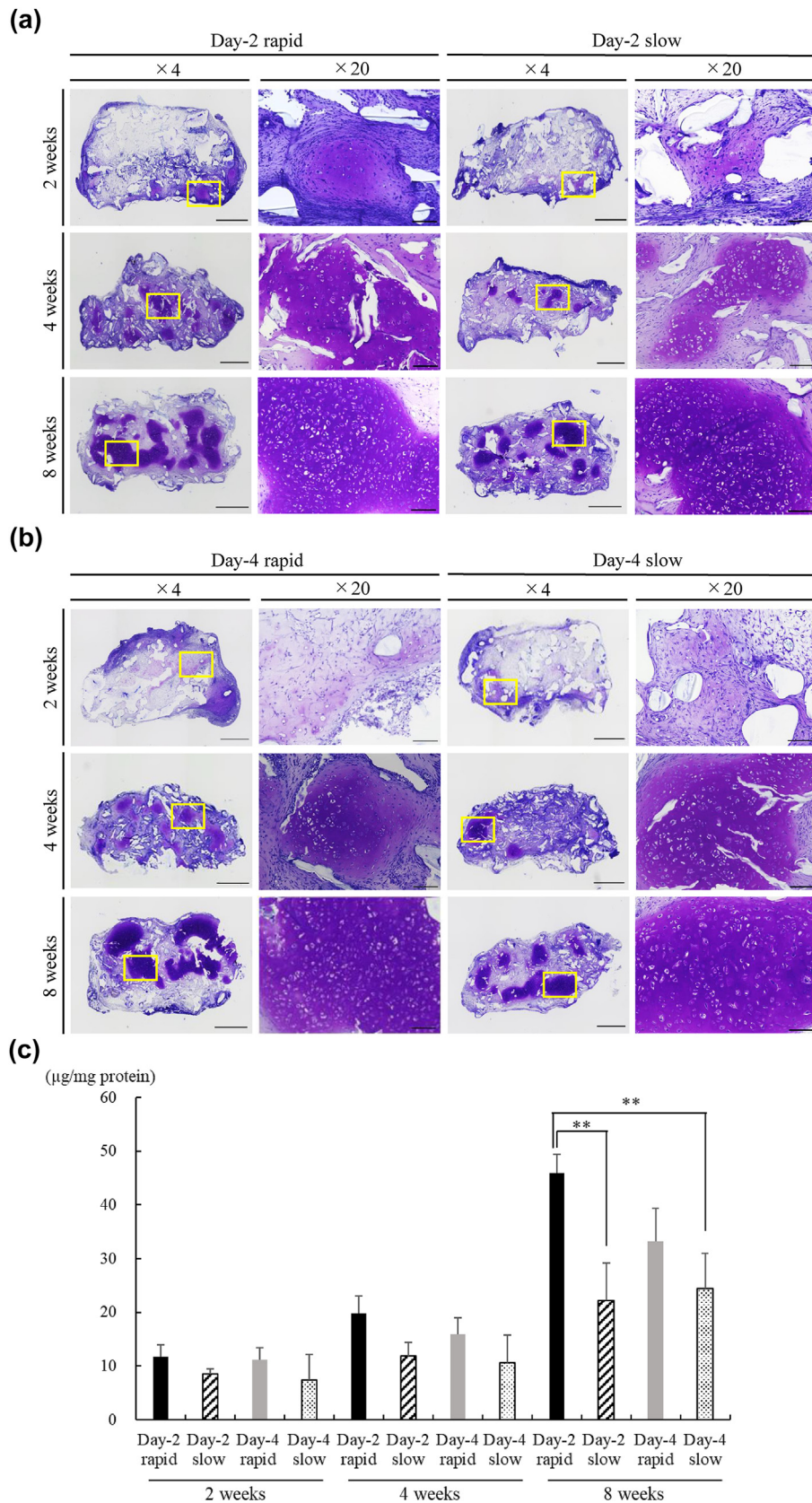


Fig. 4. Evaluation of cartilage regeneration *in vivo*. a and b. Histological analysis of implanted constructs prepared with cells sorted at day 2 (a) and day 4 (b) after CFSE staining. Histological sections were analyzed by toluidine blue staining. ×4 scale bar: 1,000 µm; ×20 scale bar: 100 µm. Yellow rectangles in the left hand columns of each group indicate the fields of view of right hand columns. c. Biochemical analysis. Accumulation of GAG 2 weeks, 4 weeks, and 8 weeks after transplantation was examined per mg total protein (n = 3, **P < 0.01).

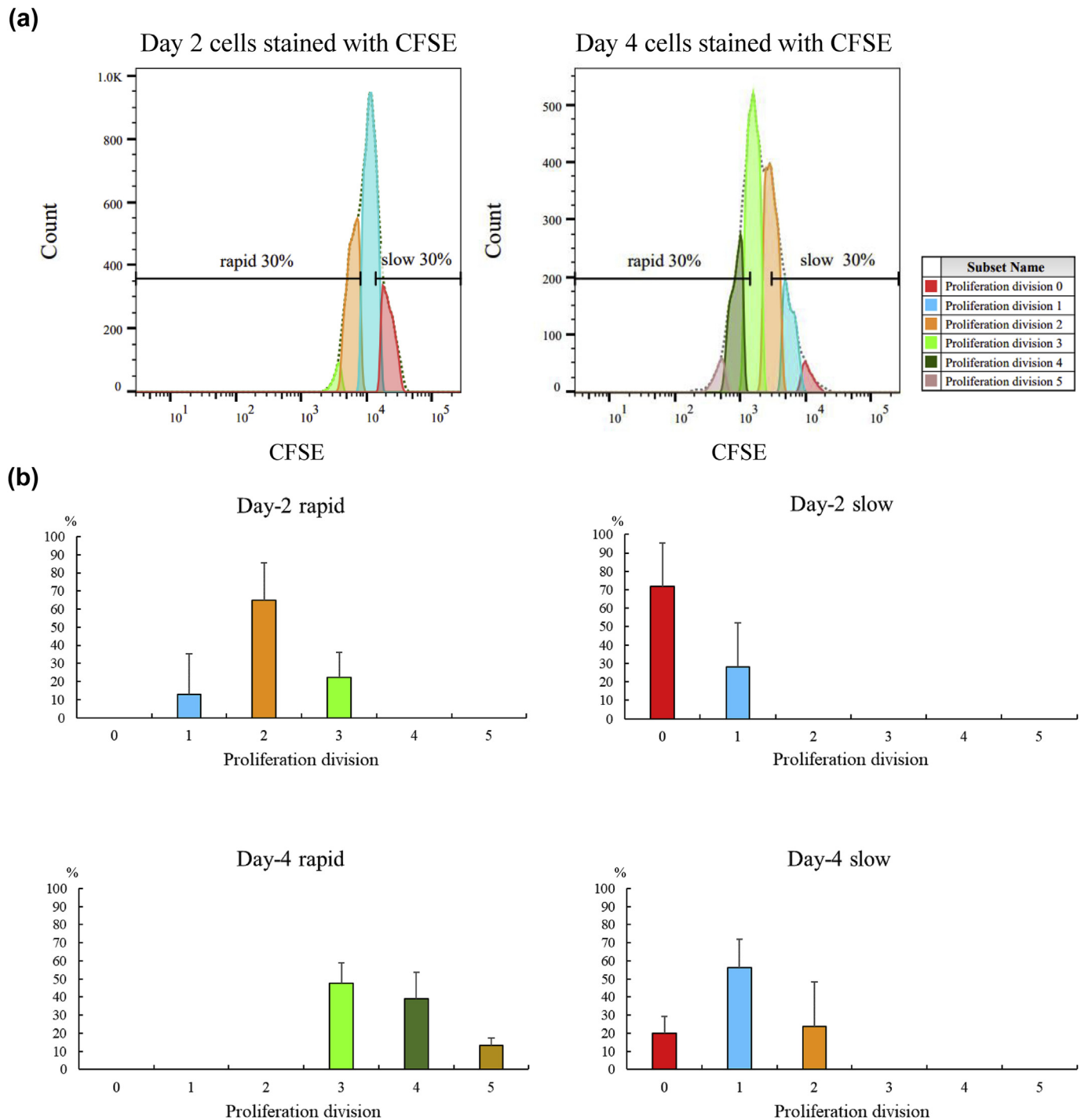


Fig. 5. Cell proliferation analysis. a. The division frequency of chondrocytes was examined on days 2 and 4 after CFSE staining. b. Numbers of cell divisions constituting the rapid and slow cell groups at days 2 and 4 after CFSE staining (n = 3).

corresponding slow groups (Figs. 2–4). The day-2 rapid group exhibited higher chondrogenic ability than the day-4 rapid group, albeit not significantly. In the *in vivo* assay, the day-2 rapid group produced significantly more GAG than the corresponding slow group, indicating successful purification of a highly chondrogenic population. These results also suggest that the cellular morphology can act as an indicator of chondrogenic capacity.

To determine the composition of the cell populations isolated 2 and 4 days post CFSE labeling, the division frequency of the cells

was analyzed. The results show that the numbers of divisions of the rapid cells from days 2 and 4 after CFSE labeling overlapped only partially (Fig. 5). Given the results of *in vivo* cartilage regeneration, in which the day-2 rapid group exhibited higher chondrogenic ability than the day-4 rapid group, it is possible that the increased number of cell divisions in the day-4 rapid group compared with the day-2 rapid group caused dedifferentiation, leading to the decline in chondrogenic capacity. Comparison of the rapid and slow cell groups harvested on days 2 and 4 showed that the rapid and

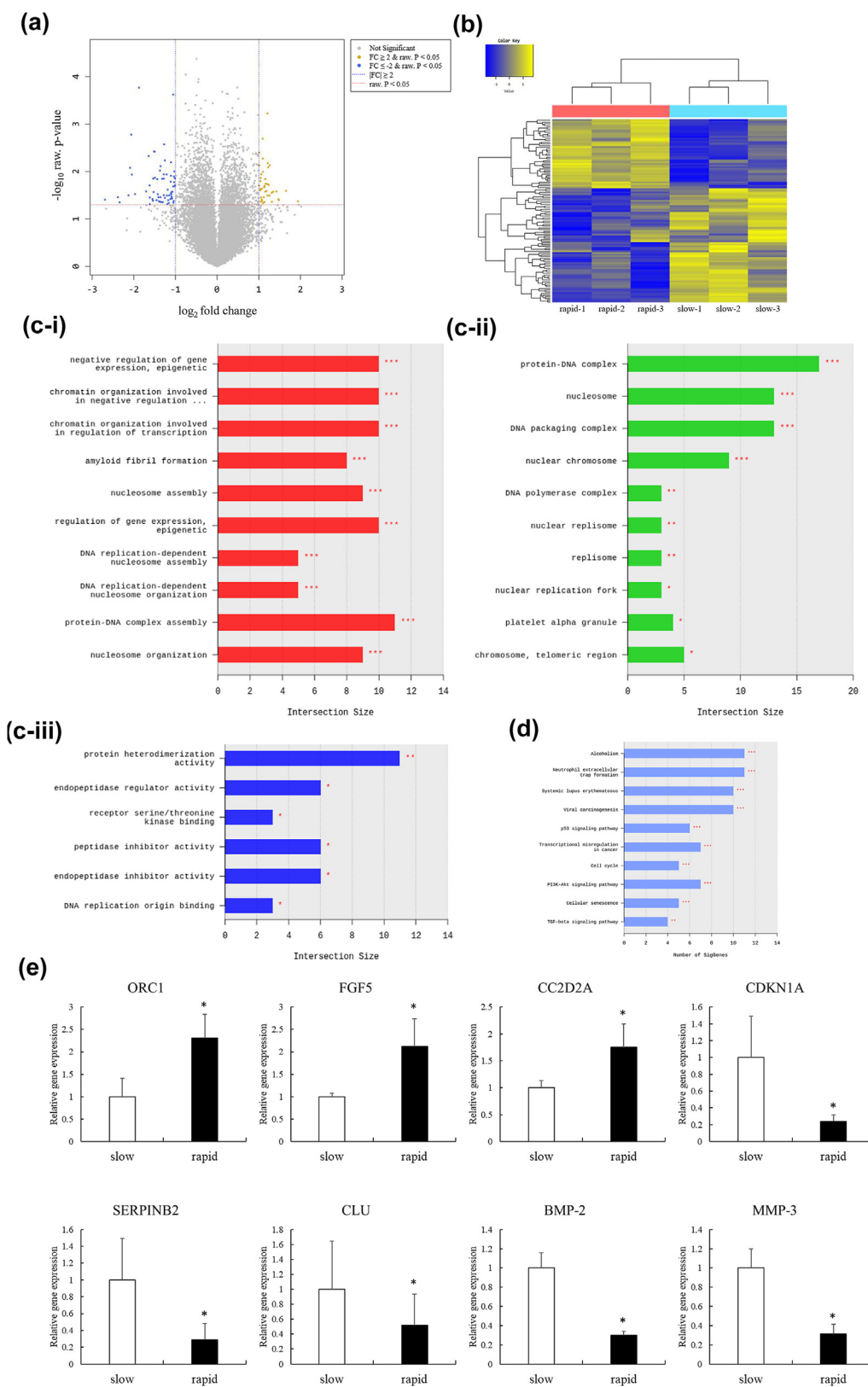


Fig. 6. Microarray analysis of the day-2 rapid and day-2 slow cell groups. a. Volcano plot. Significantly differentially expressed genes are shown based on the following criteria: |FC| ≥ 2.0 and P-value < 0.05. Orange dots represent genes that were upregulated, blue dots represent genes that were downregulated, and gray dots represent genes that were not significantly differentially expressed. b. Two-way hierarchical clustering heatmap using the z-score of the normalized value. Red labels represent the day-2 rapid group, while blue labels represent the day-2 slow group. Three different lots were analyzed. c. GO functional analysis. Three types of functional analysis are shown: biological process (i), cellular component (ii), and molecular function (iii). For biological process and cellular component the top 10 terms of GO functional analysis are shown. For molecular function the top 6 terms are shown (*P < 0.05, **P < 0.01, and ***P < 0.001). d. Top 10 terms in KEGG pathway functional analysis (**P < 0.01, ***P < 0.001). e. Real-time qPCR for differentially expressed genes identified in the microarray analysis (n = 3, *P < 0.05).

slow cell populations consisted of almost completely different cells, suggesting that cells with distinct characteristics were selected (Fig. 5).

Microarray analysis also highlighted the differences between the day-2 rapid and day-2 slow groups (Fig. 6). The results of the GO analysis confirmed that the rapid cell group contains numerous terms related to cell proliferation. Moreover, at the transcriptome level, the rapid cell group also express many genes involved in cell cycle and division, confirming the successful separation of cells according to the cell division rate.

Of the cell cycle-related genes differentially expressed in the rapid and slow cell groups, CDKN1A (also called p21), an inhibitor of cell cycle progression, was downregulated in the rapidly dividing cells. Expression of CDKN1A is low in healthy cartilage and increased in osteoarthritis cartilage [23,24]. In a previous report, cartilage pellets cultured with chondrocytes completely lacking CDKN1A produced more GAG and maintained a higher number of cells. Furthermore, colonies derived from single cells retained the potential for robust matrix production after proliferation [25]. Another study demonstrated that CDKN1A knock-down maintains the potential for GAG production even after extended passaging [26]. In our investigation, CDKN1A was downregulated in the rapid cell groups, whereas it was upregulated in the slow cell groups which have low potential for cartilage matrix production. This confirms previous findings indicating that CDKN1A is an obstacle to cartilage matrix production and regeneration.

Several genes not directly related to cell division were differentially expressed in the rapid and slow cell groups. For example, FGF5 was upregulated in the rapid cell group. This pluripotent epiblast marker is involved in stem cell maintenance and is useful in investigation of differentiation of various tissues and epiblast cells *in vivo* and *in vitro* [27–29]. Conversely, SERPINB2, CLU, BMP-2, and MMP-3 were all downregulated in the rapid cell group. In a previous study, the expression of SERPINB2 was observed to be significantly upregulated after induction of chondrogenic differentiation compared with P1 human MSCs on day 0 of differentiation. SERPINB2 may serve as a novel differentiation marker for the commitment of the MSC lineage to cartilage [30]. CLU is expressed in cartilage and its mRNA levels are significantly upregulated in osteoarthritis compared with healthy cartilage [31,32]. Furthermore, elevated levels of CLU protein have been found in the serum and synovial fluid of patients with primary osteoarthritis of the hip and knee joints [32], suggesting that CLU is a biomarker for predicting disease progression [33]. BMP-2 expression is higher in osteoarthritis cartilage than in healthy cartilage [34,35]. In fact, injection of BMP-2 into the joints of animals results in hypertrophy of articular chondrocytes and induces the formation of osteophytes, resulting in the osteoarthritis phenotype [36]. It has been reported that BMP-2 expression levels increase in cartilage and osteophytes depending on the severity of osteoarthritis [34,35,37]. The expression of MMP-3 is significantly increased in synovial tissue and peripheral blood of patients with osteoarthritis [38–40]. MMP-3, which has the ability to degrade non-collagenous matrix proteins [41], plays a central role in the degradation process of cartilage. Downregulation of these cartilage-related genes in the rapid cell group suggests that this group is more undifferentiated than the slow cell group. As mentioned above, cells with higher stemness tend to proliferate rapidly. These findings indicate that the higher chondrogenic capacity of rapid cell group described in the present report is a property of the stemness of these fast dividing cells.

The gene CC2D2A, which was not included in the KEGG pathway, was detected by the microarray analysis (i.e., $|FC| \geq 2.0$ and

P-value < 0.05). This gene has not been previously reported in relation to chondrocytes. The transition zone membrane complex, which is required for cilia formation, contains CC2D2A together with Meckel-Gruber syndrome (MKS)-Joubert syndrome (JBTS)-related proteins, such as centrosomal protein 290 (CEP290), tectonic family member 1 (TCTN1), and B9 domain containing 1 (B9D1) [42]. CC2D2A plays an essential role in the formation or stabilization of sub-basal appendages and the initiation of the process of ciliogenesis from the basal body; it is also essential for primary ciliogenesis [43]. Although few studies have been conducted on these proteins in chondrocytes, it has been reported that the expression of B9D1 is significantly reduced in osteoarthritis chondrocytes [44]. Furthermore, chondrocyte expansion and dedifferentiation are reported to inhibit primary cilia expression and Hedgehog signaling [45]. Hedgehog signaling requires primary cilia, a microtubule-based signaling compartment, whose integrity is associated with the cytoskeleton. In the present study, flow cytometric analysis showed that the cell morphology differed between the rapid and slow cell groups, as indicated by the FSC and SSC. Therefore, the difference in the expression of CC2D2A could have influenced morphology of the two groups via cilia formation. CC2D2A was abundantly expressed in the rapid cell group and hence, it could act as a new marker for cartilage matrix production in the future. Since this study was conducted only at the transcript level, the present findings should be confirmed at the protein level. Moreover, the function of CC2D2A in cartilage should be examined through the generation of knockout mice.

5. Conclusion

The present results indicate that the rapid cell group is characterized by a faster proliferation rate, smaller size, less granularity, and higher chondrogenic capacity. Microarray, GO, and KEGG analyses indicated upregulation of genes related to cell division and downregulation of several chondrocyte related genes in the rapid cell group, suggesting higher stemness of the faster dividing cells. The results obtained in this study provide the basis for the use of rapidly dividing cells in cartilage regeneration.

Funding

This study was supported by Japan Society for the Promotion of Science KAKENHI Grants-in-Aid for Scientific Research (B) (#21H03136).

Declaration of competing interest

The authors declare the following financial interests/personal relationships which may be considered as potential competing interests: Atsuhiko Hikita was affiliated with an endowed chair supported by FUJISOFT INCORPORATED (until October 31, 2020), and is affiliated with an endowed chair supported by CPC corporation, Kyowa Co., Ltd., Kanto Chemical Co. Inc., and Nichirei corporation (July 1, 2021). Yukiyo Asawa was affiliated with an endowed chair supported by Fujisoft Incorporated (until October 31, 2020). Yukiyo Asawa and Makoto Komura are affiliated with an endowed chair supported by Dental Assist Co., Ltd., Fuke Hospital, Sashiogi Hospital, Ikegami Home Clinic, and Inotec Co., Ltd.

Acknowledgments

The authors thank Ms. Dan Riu and Mr. Tomoaki Sakamoto for their technical support, and Dr. Satoru Nagata for providing us with

human auricular cartilage tissue from patients in the Nagata Microtia and Reconstructive Plastic Surgery Clinic.

Appendix A. Supplementary data

Supplementary data to this article can be found online at <https://doi.org/10.1016/j.reth.2021.12.005>.

References

- Brittberg M, Lindahl A, Nilsson A, Ohlsson C, Isaksson O, Peterson L. Treatment of deep cartilage defects in the knee with autologous chondrocyte transplantation. *N Engl J Med* 1994;331(14):889–95.
- Peterson L, Vasilopoulos HS, Brittberg M, Lindahl A. Autologous chondrocyte implantation: a long-term follow-up. *Am J Sports Med* 2010;38(6):1117–24.
- Yanaga H, Yanaga K, Imai K, Koga M, Soejima C, Ohmori K. Clinical application of cultured autologous human auricular chondrocytes with autologous serum for craniofacial or nasal augmentation and repair. *Plast Reconstr Surg* 2006;117:2019–30.
- Hoshi K, Fujihara Y, Saijo H, Kurabayashi K, Suenaga H, Asawa Y, et al. Three-dimensional changes of noses after transplantation of implant-type tissue-engineered cartilage for secondary correction of cleft lip-nose patients. *Regen Ther* 2017;7:72–9.
- Chacko S, Abbott J, Holtzer S, Holtzer H. The loss of phenotypic traits by differentiated cells. VI. Behavior of the progeny of a single chondrocyte. *J Exp Med* 1969;130(2):417–42.
- Schnabel M, Marlovits S, Eckhoff G, Fichtel I, Gotzen L, Vecsei V, et al. Dedifferentiation-associated changes in morphology and gene expression in primary human articular chondrocytes in cell culture. *Osteoarthritis Cartilage* 2002;10(1):62–70.
- Swoboda B, Holmdahl R, Stöss H, von der Mark K. Cellular heterogeneity in cultured human chondrocytes identified by antibodies specific for alpha 2(XI) collagen chains. *J Cell Biol* 1989;109(3):1363–9.
- Mantripragada VP, Tan KL, Vasavada S, Bova W, Barnard J, Muschler GF. Characterization of heterogeneous primary human cartilage-derived cell population using non-invasive live-cell phase-contrast time-lapse imaging. *Cytotherapy* 2021;23(6):488–99.
- Sebastian A, McCool JL, Hum NR, Murugesu DK, Wilson SP, Christiansen BA, et al. Single-cell RNA-seq reveals transcriptomic heterogeneity and post-traumatic osteoarthritis-associated early molecular changes in mouse articular chondrocytes. *Cells* 2021;10(6):1462.
- Häuselmann HJ, Masuda K, Hunziker EB, Neidhart M, Mok SS, Michel BA, et al. Adult human chondrocytes cultured in alginate form a matrix similar to native human articular cartilage. *Am J Physiol* 1996;271(3 Pt 1):C742–52.
- Fujihara Y, Takato T, Hoshi K. Immunological response to tissue-engineered cartilage derived from auricular chondrocytes and a PLLA scaffold in transgenic mice. *Biomaterials* 2010;31(6):1227–34.
- Asawa Y, Sakamoto T, Komura M, Watanabe M, Nishizawa S, Takazawa Y, et al. Early stage foreign body reaction against biodegradable polymer scaffolds affects tissue regeneration during the autologous transplantation of tissue-engineered cartilage in the canine model. *Cell Transplant* 2012;21(7):1431–42.
- Kobayashi S, Takebe T, Inui M, Iwai S, Kan H, Zheng YW, et al. Reconstruction of human elastic cartilage by a CD44+ CD90+ stem cell in the ear perichondrium. *Proc Natl Acad Sci U S A* 2011;108(35):14479–84.
- Hamada T, Sakai T, Hiraiwa H, Nakashima M, Ono Y, Mitsuyama H, et al. Surface markers and gene expression to characterize the differentiation of monolayer expanded human articular chondrocytes. *Nagoya J Med Sci* 2013;75(1–2):101–11.
- Xue K, Zhang X, Qi L, Zhou J, Liu K. Isolation, identification, and comparison of cartilage stem progenitor/cells from auricular cartilage and perichondrium. *Am J Transl Res* 2016;8(2):732–41.
- Diaz-Romero J, Nestic D, Grogan SP, Heini P, Mainil-Varlet P. Immunophenotypic changes of human articular chondrocytes during monolayer culture reflect bona fide dedifferentiation rather than amplification of progenitor cells. *J Cell Physiol* 2008;214(1):75–83.
- Li H, Ghazanfari R, Zacharaki D, Ditzel N, Isern J, Ekblom M, et al. Low/negative expression of PDGFR- α identifies the candidate primary mesenchymal stromal cells in adult human bone marrow. *Stem Cell Rep* 2014;3(6):965–74.
- Ishibashi M, Hikita A, Fujihara Y, Takato T, Hoshi K. Human auricular chondrocytes with high proliferation rate show high production of cartilage matrix. *Regen Ther* 2017;6:21–8.
- Kanda Y. Investigation of the freely available easy-to-use software 'EZR' for medical statistics. *Bone Marrow Transplant* 2013;48(3):452–8.
- Mabuchi Y, Morikawa S, Harada S, Niibe K, Suzuki S, Renault-Mihara F, et al. LNGFR(+)/THY-1(+)/VCAM-1(hi+) cells reveal 66 functionally distinct subpopulations in mesenchymal stem cells. *Stem Cell Rep* 2013;1(2):152–65.
- Jiang Y, Cai Y, Zhang W, Yin Z, Hu C, Tong T, et al. Human cartilage-derived progenitor cells from committed chondrocytes for efficient cartilage repair and regeneration. *Stem Cells Transl Med* 2016;5(6):733–44.
- Gherghiceanu M, Popescu LM. Cardiomyocyte precursors and telocytes in epicardial stem cell niche: electron microscope images. *J Cell Mol Med* 2010;14(4):871–7.
- Si HB, Yang TM, Li L, Tian M, Zhou L, Li DP, et al. miR-140 attenuates the progression of early-stage osteoarthritis by retarding chondrocyte senescence. *Mol Ther Nucleic Acids* 2020;19:15–30.
- Xu M, Feng M, Peng H, Qian Z, Zhao L, Wu S. Epigenetic regulation of chondrocyte hypertrophy and apoptosis through Sirt1/P53/P21 pathway in surgery-induced osteoarthritis. *Biochem Biophys Res Commun* 2020;528(1):179–85.
- D'Costa S, Rich MJ, Diekmann BO. Engineered cartilage from human chondrocytes with homozygous knockout of cell cycle inhibitor p21. *Tissue Eng Part A* 2020;26(7–8):441–9.
- Diekmann BO, Thakore PI, O'Connor SK, Willard VP, Brunger JM, Christoforou N, et al. Knockdown of the cell cycle inhibitor p21 enhances cartilage formation by induced pluripotent stem cells. *Tissue Eng Part A* 2015;21(7–8):1261–74.
- Chen E, Tang MK, Yao Y, Yau WW, Lo LM, Yang X, et al. Silencing BRE expression in human umbilical cord perivascular (HUCPV) progenitor cells accelerates osteogenic and chondrogenic differentiation. *PLoS One* 2013;8(7):e67896.
- Guzman-Ayala M, Sachs M, Koh FM, Onodera C, Bulut-Karslioglu A, Lin CJ, et al. Chd1 is essential for the high transcriptional output and rapid growth of the mouse epiblast. *Development* 2015;142(1):118–27.
- Khoa le TP, Azami T, Tsukiyama T, Matsushita J, Tsukiyama-Fujii S, Takahashi S, et al. Visualization of the epiblast and visceral endodermal cells using Fgf5-P2A-venus BAC transgenic mice and epiblast stem cells. *PLoS One* 2016;11(7):e0159246.
- Granados-Montiel J, Cruz-Lemini M, Rangel-Escareño C, Martínez-Nava G, Landa-Solis C, Gomez-García R, et al. SERPINA9 and SERPINB2: novel cartilage lineage differentiation markers of human mesenchymal stem cells with kartogenin. *Cartilage* 2021;12(1):102–11.
- Connor JR, Kumar S, Sathe G, Mooney J, O'Brien SP, Mui P, et al. Clusterin expression in adult human normal and osteoarthritic articular cartilage. *Osteoarthritis Cartilage* 2001;9(8):727–37.
- Fandridis E, Apergis G, Korres DS, Nikolopoulos K, Zoubos AB, Papassideri I, et al. Increased expression levels of apolipoprotein J/clusterin during primary osteoarthritis. *In Vivo* 2011;25(5):745–9.
- Ritter SY, Collins J, Krastins B, Sarracino D, Lopez M, Losina E, et al. Mass spectrometry assays of plasma biomarkers to predict radiographic progression of knee osteoarthritis. *Arthritis Res Ther* 2014;16(5):456.
- Nakase T, Miyaji T, Tomita T, Kaneko M, Kuriyama K, Myoui A, et al. Localization of bone morphogenetic protein-2 in human osteoarthritic cartilage and osteophyte. *Osteoarthritis Cartilage* 2003;11(4):278–84.
- Liu Y, Hou R, Yin R, Yin W. Correlation of bone morphogenetic protein-2 levels in serum and synovial fluid with disease severity of knee osteoarthritis. *Med Sci Monit* 2015;21:363–70.
- van Beuningen HM, Glansbeek HL, van der Kraan PM, van den Berg WB. Differential effects of local application of BMP-2 or TGF-beta 1 on both articular cartilage composition and osteophyte formation. *Osteoarthritis Cartilage* 1998;6(5):306–17.
- Blaney Davidson EN, Vitters EL, van der Kraan PM, van den Berg WB. Expression of transforming growth factor-beta (TGFbeta) and the TGFbeta signalling molecule SMAD-2P in spontaneous and instability-induced osteoarthritis: role in cartilage degradation, chondrogenesis and osteophyte formation. *Ann Rheum Dis* 2006;65(11):1414–21.
- Platzer H, Nees TA, Reiner T, Tripel E, Gantz S, Hagmann S, et al. Impact of mononuclear cell infiltration on chondrodestructive MMP/ADAMTS production in osteoarthritic knee joints—an ex vivo study. *J Clin Med* 2020;9(5):1279.
- Uchida K, Satoh M, Inoue G, Onuma K, Miyagi M, Iwabuchi K, et al. CD11c(+) macrophages and levels of TNF- α and MMP-3 are increased in synovial and adipose tissues of osteoarthritic mice with hyperlipidaemia. *Clin Exp Immunol* 2015;180(3):551–9.
- Li H, Li L, Min J, Yang H, Xu X, Yuan Y, et al. Levels of metalloproteinase (MMP-3, MMP-9), NF-kappaB ligand (RANKL), and nitric oxide (NO) in peripheral blood of osteoarthritis (OA) patients. *Clin Lab* 2012;58(7–8):755–62.
- Burrage PS, Mix KS, Brinckerhoff CE. Matrix metalloproteinases: role in arthritis. *Front Biosci* 2006;11:529–43.
- Garcia-Gonzalo FR, Corbit KC, Sierrol-Piquier MS, Ramaswami G, Otto EA, Noriega TR, et al. A transition zone complex regulates mammalian ciliogenesis and ciliary membrane composition. *Nat Genet* 2011;43(8):776–84.
- Veleri S, Manjunath SH, Fariss RN, May-Simera H, Brooks M, Foskett TA, et al. Ciliopathy-associated gene Cc2d2a promotes assembly of subdistal appendages on the mother centriole during cilia biogenesis. *Nat Commun* 2014;5:4207.
- Deng Z, Hu X, Alahdal M, Liu J, Zhao Z, Chen X, et al. High expression of MAPK-14 promoting the death of chondrocytes is an important signal of osteoarthritis process. *PeerJ* 2021;9:e10656.
- Thompson CL, Plant JC, Wann AK, Bishop CL, Novak P, Mitchison HM, et al. Chondrocyte expansion is associated with loss of primary cilia and disrupted hedgehog signalling. *Eur Cell Mater* 2017;34:128–41.